

RESEARCH

Open Access



Linking main ecological clusters of soil bacterial–fungal networks and nitrogen cycling genes to crop yields under diverse cropping systems in the North China Plain

Shuting Yu¹, Xinguo Chen², Tianshu Wang^{1*}, Shuihong Yao¹ and Xinhua Peng¹

Abstract

Background Crop rotation changes crop species and the associated management strategies, significantly influencing soil fertility and soil microbial communities. Interactions among the species in microbial communities are important for soil nutrient cycling. Yet, the contribution of soil microbial interactions to crop yield and soil nitrogen-cycle function under wheat–maize and wheat–soybean rotation conversion remains unclear. An 8-year field experiment was conducted to investigate the impact of simple [8-year wheat–maize rotation (8WM) and 8-year wheat–soybean rotation (8WS)] and diverse cropping systems [4-year wheat–soybean followed by 4-year wheat–maize rotation (4WS4WM) and 4-year wheat–maize followed by 4-year wheat–soybean rotation (4WM4WS)] on crop yield, soil properties, bacterial–fungal co-occurrence networks and nitrogen functional potentials. The abundances of genes with nitrogen fixation (*nifH*), nitrification (AOB and *nxrA*) and denitrification (*narG*, *nirK*, *norB* and *nosZ*) potentials were quantified and bacterial and fungal communities were characterized.

Results 4WS4WM led to higher succeeding maize yields and lower bacterial–fungal network complexity, nitrogen fixation potentials and denitrifying potentials than 8WM. Meanwhile, 4WM4WS exhibited higher succeeding wheat and soybean yields, network complexity and lower nitrifying potentials than 8WS. The ecological cluster with the most nitrifying and denitrifying bacterial species (Module#5) and that with the least species (Module#3) dominated the potentials of nitrogen fixation, nitrification and denitrification and succeeding maize yields in 4WS4WM and 8WM. Module#4 with the highest abundances of nitrifying bacteria (*Nitrosomonadaceae*) and Module#2 with the most species dominated the nitrifying potentials and succeeding wheat and soybean yields in 4WM4WS and 8WS. Soil water content, organic carbon, dissolved organic carbon, NO_3^- and pH were key drivers influencing Module#3 and Module#5, while only NH_4^+ significantly affected Module#2 and Module#4.

Conclusions These findings demonstrate the importance of ecological clusters within soil microbial network in regulating crop yield and soil nitrogen cycling, and identify specific ecological clusters dominating nitrogen functional potentials in wheat–maize and wheat–soybean rotations, offering science-based recommendations for sustainable crop rotation practices.

Keywords Crop rotation, Bacterial–fungal co-occurrence network, Nitrogen functional potentials, Crop yield

*Correspondence:

Tianshu Wang
wangtianshu@caas.cn

Full list of author information is available at the end of the article



© The Author(s) 2024. **Open Access** This article is licensed under a Creative Commons Attribution-NonCommercial-NoDerivatives 4.0 International License, which permits any non-commercial use, sharing, distribution and reproduction in any medium or format, as long as you give appropriate credit to the original author(s) and the source, provide a link to the Creative Commons licence, and indicate if you modified the licensed material. You do not have permission under this licence to share adapted material derived from this article or parts of it. The images or other third party material in this article are included in the article's Creative Commons licence, unless indicated otherwise in a credit line to the material. If material is not included in the article's Creative Commons licence and your intended use is not permitted by statutory regulation or exceeds the permitted use, you will need to obtain permission directly from the copyright holder. To view a copy of this licence, visit <http://creativecommons.org/licenses/by-nc-nd/4.0/>.

alter the co-occurrence patterns of microbes [25]. Furthermore, the ecological clusters in microbial co-occurrence networks can be linked to the positive regulation of soil carbon, nitrogen, phosphorus, and sulfur cycling functional genes [10]. However, there is still a lack of understanding of crop rotation regarding the regulation of specialized ecological clusters on soil nutrient cycling and crop yield.

Crop rotation systems can select specialized soil functional microbes through species-specific root exudation and preceding crop residue inputs [26, 27]. In simple two-crop rotations, each plant type seasonally shapes the soil bacterial and fungal communities through rhizodeposition and crop residue decomposition [28, 29]. For example, wheat–maize rotations have been shown to selectively enrich copiotrophic bacteria and stubble-borne pathogens like *Fusarium* and *Rhizoctonia* due to the higher residue and fertilizer inputs, concurrently reducing *nifH* abundance [14, 30]. Rotations with legumes tend to augment diazotrophic and nitrifying bacterial populations as well as saprophytic fungi [31–33]. Considering crop rhizosphere is the hot spot for soil nutrient cycling, understanding how crop rotation systems modulate soil nitrogen cycling by regulating the rhizosphere microbial community is the key to promoting plant productivity [28, 34].

Here, we applied 16S and ITS2 amplicon sequencing and quantitative PCR (qPCR) technologies to address the abovementioned knowledge gaps on an 8-year diverse cropping experiment [two diverse cropping systems (4-year wheat–soybean followed by 4-year wheat–maize (4WS4WM), and 4-year wheat–maize followed by 4-year wheat–soybean (4WM4WS)], and two simple rotations [8-year wheat–maize rotation (8WM), and 8-year wheat–soybean rotation (8WS)] in North China Plain. The objectives of this study were (i) to identify the main ecological clusters and nitrogen functional taxa within the bacterial–fungal co-occurrence network under diverse rotation systems; (ii) to clarify the effects of preceding crop rotation on the process of nitrogen–fixation, nitrification, and denitrification in succeeding wheat–maize and wheat–soybean soil; and (iii) to explore the relationship between the ecological clusters and nitrogen functional genes and their contributions to succeeding crop yield. We hypothesized: (i) the preceding rotation alters the complexity and main ecological clusters of bacterial–fungal co-occurrence network in succeeding wheat–maize and wheat–soybean soil; (ii) the preceding rotations show different nitrogen-cycle processes in succeeding wheat–maize and wheat–soybean soil; and (iii) soil nitrogen function and crop productively are driven by different ecological clusters in succeeding wheat–maize and wheat–soybean soil.

Materials and methods

Site description and experimental design

A long-term diverse crop rotational experiment was initiated in 2013 at the experimental station of the Farmland Irrigation Research Institute, Chinese Academy of Agricultural Sciences, Xinxiang City of Henan Province (35°19' N, 113°53' E). This site has a typical warm temperate continental monsoon climate with a mean annual temperature of 14.0 °C and precipitation of 573.4 mm. The experimental soil is derived from alluvial sediments of the Yellow River and is classified as Aquic Ustochrept according to U.S. soil taxonomy. The soil type was a sandy loam texture with 53.1% sand, 43.1% silt, and 3.8% clay. Before the experiment, winter wheat–summer maize rotation with regular chemical fertilizer inputs had been carried out in this experimental area for four decades. From mid-October to early June, winter wheat was planted with the application of 255 kg ha⁻¹ of nitrogen (N), 112.5 kg ha⁻¹ of phosphate (P₂O₅), and 75 kg ha⁻¹ of potassium (K₂O). The growing season for summer maize was from early June to early October, with the application of 180 kg ha⁻¹ of nitrogen, 90 kg ha⁻¹ of phosphate (P₂O₅), and 120 kg ha⁻¹ of potassium (K₂O). Urea (46% N), calcium superphosphate (16% P₂O₅), and potassium chloride (60% K₂O) were used as the sources of nitrogen, phosphate, and potassium fertilizers, respectively. The soil at 0–20 cm contains 16.0 g kg⁻¹ organic carbon (SOC), 1.51 g kg⁻¹ total nitrogen (TN), 52.5 mg kg⁻¹ mineral nitrogen, 28.8 mg kg⁻¹ available phosphorus (AP), 264 mg kg⁻¹ exchangeable potassium (AK), and a bulk density of 1.43 g cm⁻³ at the beginning of the long-term experiment.

The experimental design was a randomized complete block with four replications of two treatments before the cropping system conversion in 2017. The two cropping systems established in October 2013 were continuous cropping of winter wheat (*Triticum aestivum* L.) sequenced with summer maize (*Zea mays* L.) (8WM) and summer soybean (*Glycine max* L.) (8WS), with the plot area of 102 (6 m × 17 m) m². To further illustrate the influence of preceding crop rotation and crop rotational diversity on soil fertility and subsequent crop productivity, each plot was split in half in June 2018, with one half using summer maize replacing summer soybean, resulting in a new system of 4WS4WM) and vice versa, resulting in another new system (4WM4WS) (Fig. S1). There are four rotation schemes in total: (1) 8-year simple inner-year wheat–maize rotation (8WM); (2) 8-year simple inner-year wheat–soybean rotation (8WS); (3) 4-year wheat–soybean rotation followed by 4-year wheat–maize rotation (4WS4WM); and (4) 4-year wheat–maize rotation followed by 4-year wheat–soybean rotation (4WM4WS). Two crops in a rotational sequence are

present each year. Wheat was planted in early October and harvested in early June of the next year, and maize or soybean was planted in early June and harvested in early October. The seeding rate of wheat (cv Zhoumai 22) was 225 kg ha⁻¹ (the plant populations were about 1.82 × 10⁶ plants ha⁻¹), with 20 cm between rows. Maize (cv Zhengdan 958) was sowed at 37.5 kg ha⁻¹ of seeds, with 60 cm between rows and 25 cm between plants in rows. Soybean (cv Zheng 1307) were sowed at 75 kg ha⁻¹ of seeds, with 40 cm between rows and 11 cm between plants in rows. Rate and species of fertilizations, tillage, pest control and irrigation were described in detail in previous publications [31, 35]. The grain yields of wheat, maize, and soybean under each rotation system were recorded in 2014–2021 in Fig. S2. After crop rotation conversion, 4WS4WM significantly increased the 4-year average maize yield by 16.5%, and 4WM4WS markedly increased the 4-year average yields of wheat and soybean by 13.1% and 29.2%, respectively.

Soil sampling and analysis

Rhizosphere soil samples were collected at the soybean full bloom stage or maize silking stage (August 10, 2021) after a cycle of 8-year rotations to study the cumulative impact of long-term crop rotation. Soybean plants were at the full bloom stage and maize plants at the silking stage, which corresponded to the peak root size, architectural development, and nitrogen fixation activity of soybean plants [36, 37]. Two plants were randomly removed from the ground at a depth of 20 cm in each plot, shaken off the loosely adhered soil, and collected the soil that was tightly attached to the surface of plant roots. Two plant samples were pooled together as a composite sample in each plot avoiding border effects. In total, 16 soil samples (4 rotation systems × 4 replicates) were stored in polyethylene bags and immediately transported to the laboratory on dry ice packs (– 20 °C). After removing fine litter, root residues, and stones, soil samples were divided into three parts. One part was stored at – 20 °C for DNA extraction, one was immediately stored at 4 °C for the determination of contents of soil water (SWC), pH, ammonia (NH₄⁺), and nitrate (NO₃⁻) contents, and the remaining soil was air-dried and sieved to determine soil SOC, dissolved organic carbon (DOC), TN, AP and AK. SWC was measured using the oven-drying method. Soil pH in water (soil to water 1:2.5) was measured by a pH meter (Thermo Orion-868). SOC and TN were determined with an element analyzer (Vario MACRO Cube, Elementar, Germany) after removing inorganic C. DOC was extracted using distilled water (1:10 w/v soil-to-water ratio), and determined using a total organic carbon analyzer (Multi-N/C 2100, Analytik Jena AG, Germany) [38]. NH₄⁺ and NO₃⁻ were extracted by 2 mol L⁻¹ potassium

chloride, and determined by a continuous flow autoanalyzer (Seal Auto Analyzer 3-AA3, Seal Analytical) [39]. AP was extracted by 0.5 mol L⁻¹ sodium bicarbonate and determined with the molybdenum blue method [40]. AK was read by flame photometry (6400A, INESA, China) following extraction with 1 mol L⁻¹ ammonium acetate [41].

Soil DNA extraction, amplicon sequencing, and sequence analysis

Soil microbial DNA was extracted from 0.5 g of fresh soil using NucleoSpin[®] Soil (Macherey–Nagel). The 16S rDNA gene V3–V4 region (16S) for bacteria was amplified using primers 338F (ACTCCTACGGGAGGC AGCA) and 806R (GGACTACHVGGGTWTCTAAT). The internal transcribed spacer 2 (ITS2) for fungi was amplified using primers ITS7F (GTGARTCATCGA RTCTTTG) and ITS4R (TCCTCCGCTTATTGATAT GC). Pair-end 2 × 250 bp sequencing was performed using the Illumina NovaSeq platform at Shanghai Personal Biotechnology Co., Ltd (Shanghai, China). The raw sequences were deposited at the NCBI Sequence Read Archive (SRA) with the accession number PRJNA989763.

Bacterial and fungal amplicon sequences were processed using the QIIME2 pipeline (version 2018.11, <https://qiime2.org>). Raw amplicon reads were merged, and then primers, barcodes and low-quality sequencing read with an average base quality score < 20 and sequence length < 50 bp were removed. The high-quality sequences were denoised into amplicon sequence variants (ASVs) and representative sequences were picked at 97% sequence similarity using the DADA2 plugin [42]. Bacterial and Fungal ASVs were taxonomically assigned with the SILVA database and UNITE (v8.0) database, respectively. Sequencing libraries were rarefied to the smallest library size for each sample group, and 32,768 reads for 16S and 68,072 reads for ITS were used for soil libraries.

Real-time qPCR and nitrogen functional potentials calculations

The copy numbers of bacterial 16S rDNA gene and seven nitrogen functional genes (*nifH*, bacterial *amoA* (AOB), *nxrA*, *narG*, *nirK*, *norB* and *nosZ*) of all soil samples ($n=16$) were quantified using a 7500 Real-Time PCR System (Applied Biosystems, Foster City, CA, USA), based on the degenerate primer sets detailed in Table S1. Each 20 μL PCR reaction system included 1 μL template DNA, 10 μL SYBR Premix Ex Taq II (Tli RNaseH Plus; 2 ×; Takara Bio Inc. Shiga, Japan), 0.4 μL (10 μM) of each primer, and 8.2 μL nuclease-free water. Sterilized water was used as the negative control in each qPCR run. All samples were analyzed three times in parallel. PCR runs were started with an initial denaturation for 5 min at 95

°C, followed by 40 cycles of 15 s at 95 °C, and 30 s at 60 °C. All runs had standard efficiency curves of $R^2 > 0.99$, efficiencies of 86–96%, and no template controls resulted in null or negligible values. The specificity of PCR products was determined by the melting curve. The number of gene copies per gram dry soil of sample (C, copies/g dry soil) was calculated.

Soil total nitrogen functional potentials were calculated by averaging the normalized (Z-score transform) seven nitrogen functional genes. Meanwhile, *nifH* was Z-score transformed to soil nitrogen fixation potentials. Nitrification potentials were calculated by averaging the normalized AOB and *nxrA*, and denitrification potentials were calculated by averaging the normalized *narG*, *nirK*, *norB* and *nosZ*.

Co-occurrence network analysis and functionality prediction

We constructed a total co-occurrence network with all the samples to visualize correlations between bacteria and fungi using *corAndPvalue* function of the WGCNA package based on Spearman's rank analysis [43]. The ASVs with more than 80% of the relative abundance for bacteria (2145 ASVs) and fungi (53 ASVs) in all samples were merged into an abundance table to construct the co-occurrence network as previous studies described [10, 11]. Only the edges with a Spearman correlation higher than 0.6 and adjusted *P* values lower than 0.05 were retained. The main ecological clusters in the network were visualized with the Gephi (<https://gephi.org/>) [44]. The relative abundance of each module was the cumulative relative abundance of the species that belong to it [45]. The sub-network topological parameters of each rotation treatment were extracted from the total co-occurrence network by the *igraph* package, and then calculated topological properties of each network (average degree, closeness centrality, betweenness centrality, and modularity). Soil bacterial and fungal functional communities were predicted using the Functional Annotation of Prokaryotic Taxa (FAPROTAX) and FUNGuild v1.0 (<https://github.com/UMNFuN/FUNGuild>), respectively [46, 47]. To quantitatively assess the contribution of bacteria involved in the nitrogen cycle in each module, the absolute abundances of bacteria involved in nitrogen fixation, nitrification, and denitrification were calculated by multiplying the total bacterial abundance by their relative abundances in each module [48].

Statistical analysis

All statistical analyses and visualizations were performed in R 3.6.1. Principal coordinate analysis (PCoA) [49] was performed to determine the effects of the cropping systems on bacterial and fungal composition based on the

Bray–Curtis distance matrix of the ASVs. A one-way ANOVA with Tukey's HSD test in the *agricolae* package was used to compare the abundances of bacteria, nitrogen functional genes, and main modules in bacterial–fungal co-occurrence networks, total nitrogen functional potentials, nitrogen fixation potentials, nitrification potentials and denitrification potentials between different rotation treatments at $P < 0.05$. Principal component analysis (PCA) of the soil nitrogen functional genes was performed to determine the variability of the soil nitrogen functional communities among the different rotation treatments. PCA was interpreted graphically by constructing bi-plots, with factor scores to specify the loadings of individual functional genes on the first two principal components. The regression analysis was conducted on the relationship of the bacterial–fungal network module with nitrogen functional potentials and genes using the *lme4* package. Pearson correlation analysis was performed using the *Hmisc* package to identify the significant correlations of soil physicochemical properties and abundances of nitrogen functional genes and bacterial–fungal network module, and nitrogen functional potentials [50]. The relationships between crop yield and nitrogen functional potentials were also analyzed by Pearson correlations. The associations of crop yield, nitrogen functional potentials and bacterial–fungal network module were estimated by the Mantel test [51].

Results

Microbial co-occurrence network characters

The Venn diagrams showed different patterns of bacterial and fungal total ASVs and unique ASVs among four cropping systems (Fig. 1A). Bacterial and fungal ASVs ranged from 7126–7585, and 666–714, respectively, with the highest total ASVs and unique ASVs in 8WM. Under the subsequent wheat–maize rotation, the bacterial and fungal total ASVs and unique ASVs were lower in 4WS4WM than in 8WM. Under the subsequent wheat–soybean rotation, the bacterial total and unique ASVs were lower in 4WM4WS than in 8WS, while the fungal total and unique ASVs were opposite. Four cropping systems had shared 1752 bacterial and 227 fungal ASVs, respectively. The community composition of bacteria (PERMANOVA, $R^2 = 0.34$, $P < 0.001$) and fungi (PERMANOVA, $R^2 = 0.46$, $P < 0.001$) in four cropping systems were clearly separated from each other based on Principal coordinate analysis (Fig. S3).

Co-occurrence patterns of bacteria and fungi in all samples were determined using the network analysis based on Spearman's correlation between ASVs ($R > 0.80$; $P < 0.05$) (Fig. 1B). The overall network comprised 1020 nodes, 1265 edges and 7 main ecological clusters (Module#1–7), with 95.4% of edges between bacteria and

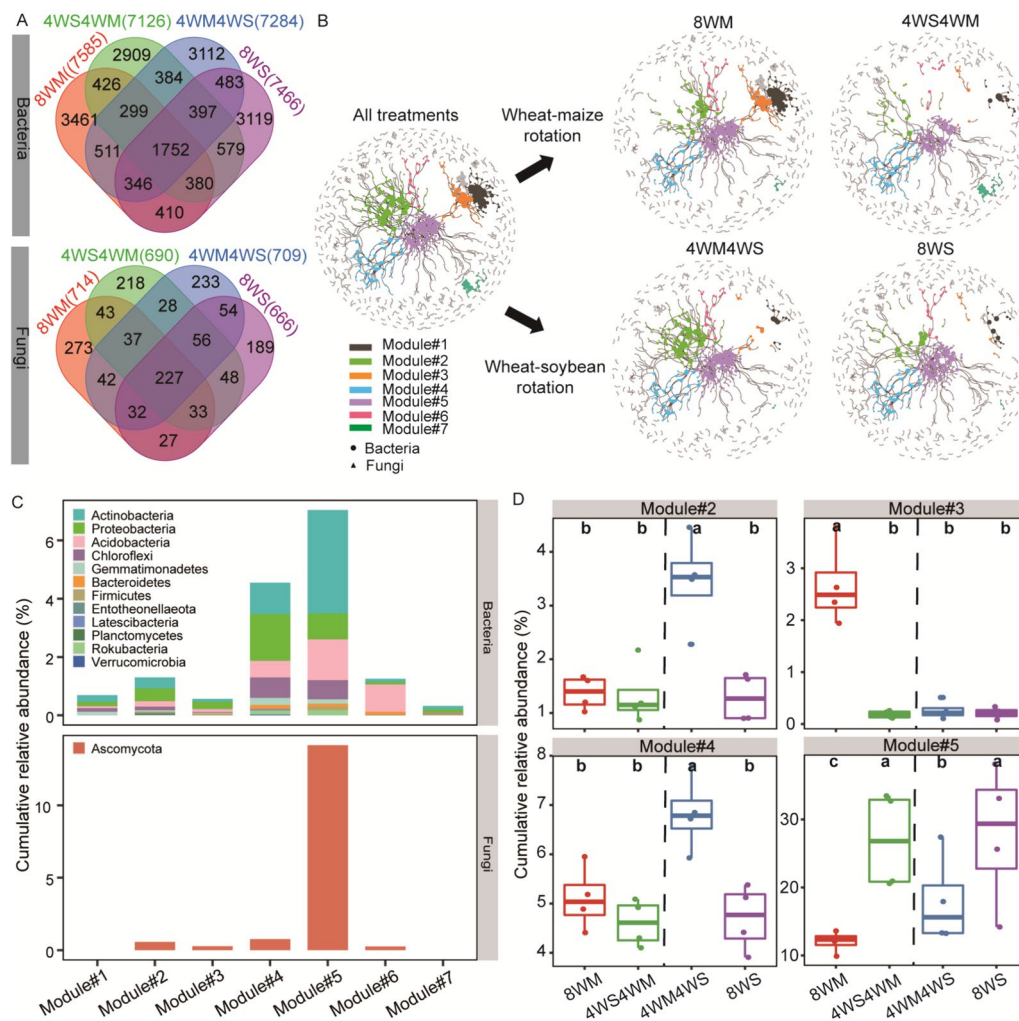


Fig. 1 Bacterial and fungal community and their inter-kingdom co-occurrence network. **A** Venn diagrams indicate numbers of unique and shared non-singleton amplicon sequence variants (ASVs) in different cropping systems. **B** Bacterial-fungal network and sub-networks in different cropping systems. Each edge stands for a strong ($R > 0.8$) and significant correlation ($P < 0.05$). Nodes are colored according to seven ecological clusters (Modules#1–7). **C** Relative abundance of bacterial and fungal phyla in the main modules. **D** Relative abundance of the main modules in different cropping systems. Different lowercase letters indicate the values that differ significantly among treatments at $P < 0.05$. 8WM 8-year simple wheat–maize rotation, 8WS 8-year simple wheat–soybean rotation, 4WS4WM 4-year wheat–soybean followed by 4-year wheat–maize rotation, 4WM4WS 4-year wheat–maize followed by 4-year wheat–soybean rotation

4.20% between bacteria and fungi (Table 1). The sub-network results shows that the complexity (a higher average degree representing a greater network complexity) and positive bacterial inter-interactions of 4WS4WM were lower than 8WM, while those of 4WM4WS were higher than 8WS. Relative abundances of 7 main ecological clusters were in order: Module#5 (84.7%) > Module#4 (21.2%) > Module#2 (7.40%) > Module#6 (6.00%) > Module#3 (3.30%) > Module#1 (2.80%) > Module#7 (1.30%) (Fig. 1C). Module#2–5 consisted of more bacterial and fungal phyla than Module#1, Module#6 and Module#7. Module#2 included the most bacterial phyla (11, except

for *Verrucomicrobia*), and Module#5 contained the 8 bacterial phyla and fungal phylum *Ascomycota* with the highest relative abundances. Module#3 and Module#5 abundances were more sensitive to preceding rotation system under subsequent wheat–maize rotation than other modules, and the relative abundances of Module#3 were lower 93% in 4WS4WM than in 8WM, and those of Module#5 were higher 1.23-fold (Fig. 1D). Module#2 and Module#4 abundances were more sensitive to preceding rotation system under subsequent wheat–soybean rotation than other modules, and the relative abundances of Module#2 and Module#4 were higher 1.68-fold and

Table 1 Topological properties of bacterial–fungal network and the sub-networks in different cropping systems in the 8th year of rotation

	All treatments	8WM	4WS4WM	4WM4WS	8WS
Node	1020	816	749	779	797
Edge	1265	932	666	823	734
Positive edge	1060 (83.8%)	750 (80.5%)	501 (75.2%)	651 (79.1%)	551 (75.1%)
Negative edge	205 (16.2%)	182 (19.5%)	165 (24.8%)	172 (20.9%)	183 (24.9%)
Bacteria–Bacteria					
Positive edge	1024 (80.9%)	720 (77.3%)	475 (71.3%)	622 (75.6%)	521 (71.0%)
Negative edge	183 (14.5%)	160 (17.2%)	147 (22.1%)	151 (18.3%)	161 (21.9%)
Bacteria–Fungi					
Positive edge	33 (2.6%)	27 (2.9%)	23 (3.5%)	26 (3.2%)	27 (3.7%)
Negative edge	20 (1.6%)	20 (2.1%)	16 (2.4%)	19 (2.3%)	20 (2.7%)
Fungi–Fungi					
Positive edge	3 (0.2%)	3 (0.3%)	3 (0.5%)	3 (0.4%)	3 (0.4%)
Negative edge	2 (0.2%)	2 (0.2%)	2 (0.3%)	2 (0.2%)	2 (0.3%)
Degree	2.48	2.28	1.78	2.11	1.84
Eccentricity	8.62	7.39	5.11	7.54	6.62
Closeness centrality	0.49	0.49	0.57	0.51	0.54
Betweenness centrality	890	576	187	489	378
Modularity	58.2	83.9	84.3	83.6	100

45% in 4WM4WS than in 8WS. The nodes of Module#2, Module#3, Module#4, and Module#5 across different rotation treatments were dominated by bacteria (92.3–100%) (Fig. 2). 4WS4WM showed the least species in Module#3 than the other modules, whereas 4WM4WS had the most species in Module#2.

Bacterial nitrogen functional and plant pathogenic nodes in main modules

Eleven bacterial nitrogen functional nodes with nitrification (7 nodes) and denitrification (4 nodes) were found in Module#2, Module#4, and Module#5, and were calculated their absolute abundances based on the total bacterial abundance (Figs. 3 and S4). The changes in relative abundance and absolute abundance of nitrogen functional groups were similar between treatments (Fig. S5). Compared to 8WM, 4WS4WM induced higher absolute abundances of nitrifying *Ellin6067_ASV218* (Family *Nitrosomonadaceae*) in Module#4 and denitrifying *Stenotrophomonas_ASV2184* in Module#2, and resulted in lower absolute abundances of nitrifying *MND1_ASV416* (Family *Nitrosomonadaceae*), denitrifying *Bacillus_ASV300*, and *Rubrobacter_ASV56* in Module#5. Meanwhile, the absolute abundances of nitrifying *Nitrosomonadaceae* (*MND1_ASV3* and *Ellin6067_ASV218*) in Module#4 were higher and denitrifying *Bacillus_ASV300* and *Rubrobacter_ASV56* in Module#5 were lower in 4WM4WS than in 8WS.

For fungal functional groups, two plant pathogenic nodes and seven saprotrophic nodes were detected using the FUNGuild annotation tool (Table 2). The relative abundance of pathogenic *fungi_ASV52* (*Alternaria*, 0.98%) in Module#5 was the highest in 4WS4WM. 4WM4WS showed the lowest relative abundances of pathogenic *fungi_ASV22* (*Fusarium*, 0.22%) in Module#2 and the highest those of pathogenic *fungi_ASV34* (*Gibellulopsis*, 1.34%) and saprotrophic *fungi_ASV19* (*unclassified_Microascaceae*, 0.95%). These values in 4WM4WS had significant differences with the other three treatments. In addition, the relative abundances of saprotrophic *fungi_ASV1* (*Botryotrichum*), *fungi_ASV18* (*Botryotrichum*) and *fungi_ASV19* (*unclassified_Microascaceae*) in Module#5 were also higher in 4WS4WM than in 8WM.

Soil nitrogen functional genes and potentials

We investigated the effects of diverse cropping systems on soil nitrogen functional genes and potentials over an 8-year rotational cycle (Fig. 4). The principal component analysis (PCA) demonstrated changes in soil nitrogen-cycle microbial communities among the four treatments (Fig. 4A). The first two principal components (PC1 and PC2) explained 68.91% of the total variance, separating the diverse cropping system communities (4WS4WM, 4WM4WS) from 8WM and 8WS communities along PC1 and PC2, respectively. Their nitrogen functional communities were significantly

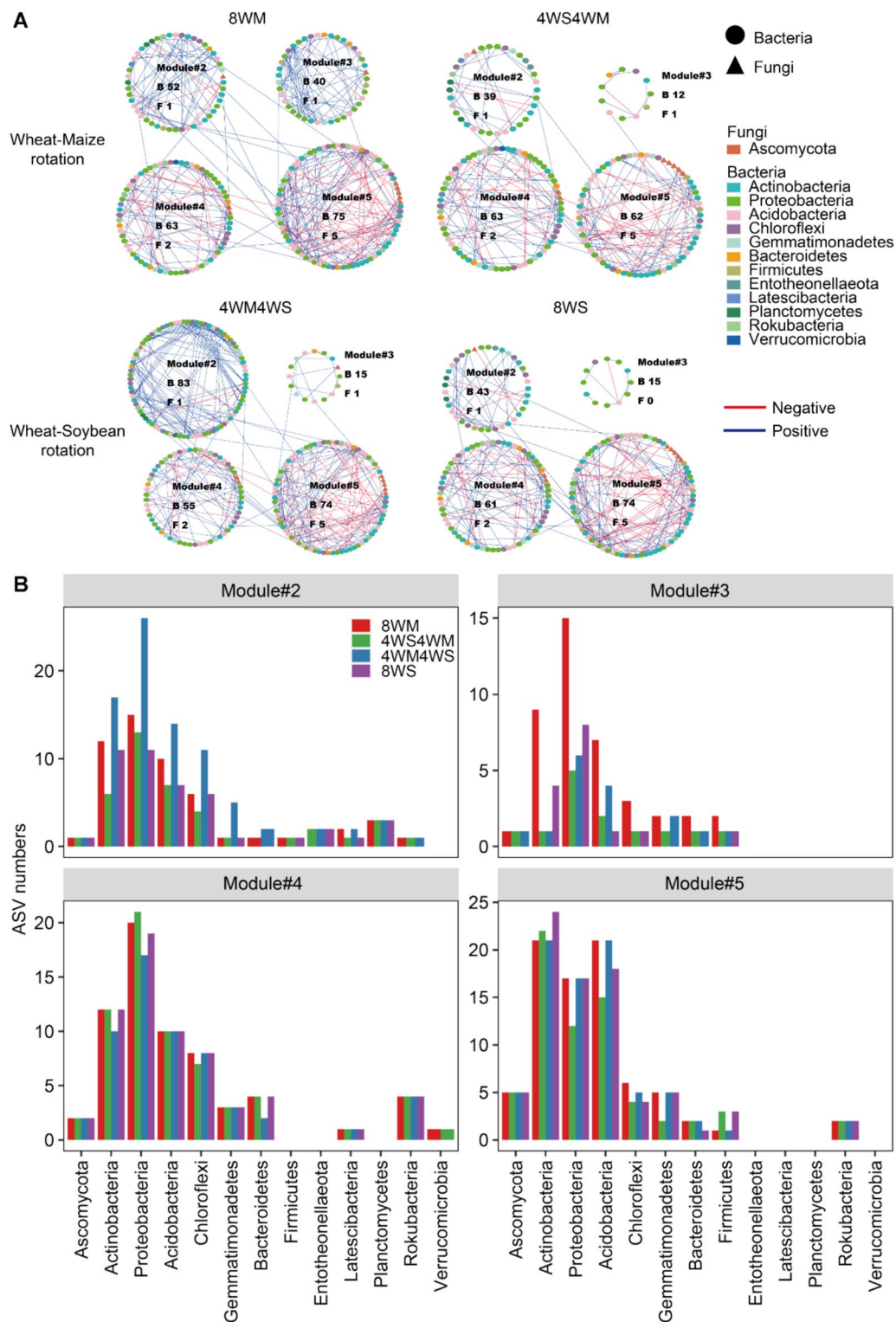


Fig. 2 Main ecological cluster patterns (A) and their non-singleton amplicon sequence variants (ASVs) numbers at the phylum level (B) within bacterial-fungal networks across different rotation treatments. The colours of nodes indicate different phyla. The blue and red edges indicate positive and negative correlations between two individual nodes, respectively

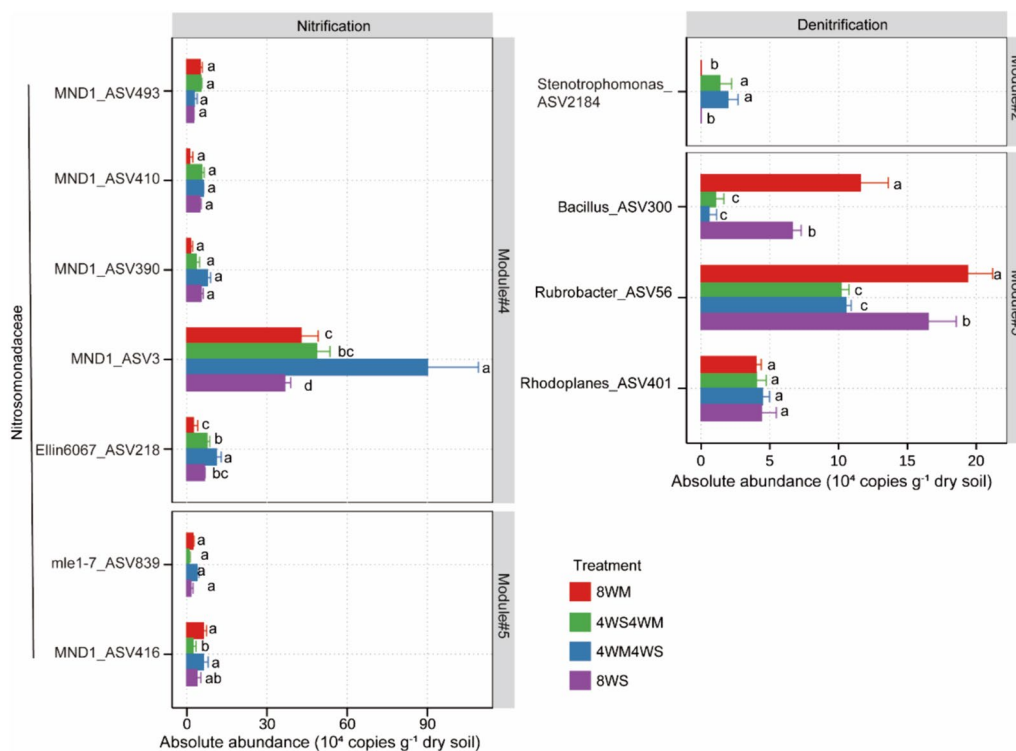


Fig. 3 Absolute abundances of bacterial taxa with nitrification and denitrification in main modules across different rotation treatments. Different lowercase letters indicate the values that differ significantly among treatments at $P < 0.05$

separated from 8WM and 8WS via PC1. The shifts of the community composition via PC1 and PC2 were driven by the *nifH* for nitrogen fixation, *norB*, *narG* and *nosZ* genes for denitrification associated with the 8WM and by the AOB, and *nxrA* genes for nitrification associated with the 8WS. Specifically, the abundances of *nifH*, *nirK* and *nosZ* genes were significantly lower in 4WS4WM than in 8WM, while those of AOB and *nxrA* genes showed an opposite pattern (Fig. 4B). In contrast, the abundances of AOB, *nxrA*, and *nirK* genes were significantly lower in 4WM4WS than in 8WS, while those of *narG* were significantly higher. These functional genes are further transformed into functional potentials of nitrogen fixation, nitrification, and denitrification processes (Fig. 4C). 4WS4WM resulted in a decline in total nitrogen functional potentials due to the lower nitrogen fixation (1.87-fold) and denitrification potentials (90.0%) relative to 8WM (Fig. 3A). The nitrification potentials were significantly higher by 1.01-fold in 4WS4WM than in 8WM. The nitrification and total nitrogen functional potentials were significantly lower in 4WM4WS than in 8WS, while other potentials were comparable.

Bacterial–fungal network modules linking to soil nitrogen functional potentials

The regression analysis showed the relative abundance of Module#2 ($R^2 = 0.26$, $P = 0.04$) and Module#4 ($R^2 = 0.37$, $P = 0.01$) all negatively correlated with soil total nitrogen functional potentials, and those of Module#3 ($R^2 = 0.33$, $P = 0.02$) positively correlated with soil total nitrogen functional potentials (Fig. 5). The relative abundance of Module#5 positively correlated with soil nitrification potentials ($R^2 = 0.31$, $P = 0.03$), and negatively correlated with soil denitrification potentials ($R^2 = 0.28$, $P = 0.03$). In addition, relative abundances of Module#2 and Module#4 negatively correlated with AOB, but those of Module#5 showed an opposite pattern (Fig. S6). Significant negative relationships were found between Module#2 and *nirK* and *nosZ*, Module#3 and *nxrA*, Module#5 and *norB*.

Abundances of bacterial–fungal network modules and nitrogen functional potentials correlated with soil physicochemical properties

The relationships between the bacterial–fungal network module, nitrogen function, and soil physicochemical properties were further analyzed by Pearson correlation

Table 2 Relative abundance (%) of fungal functional taxa in Module#2, Module#3, Module#4 and Module#5 across different rotation treatments

ASV	Class	Order	Family	Genus	Module	Function	8WM	4WS4WM	4WM4WS	8WS
fungi_ASV22	Sordariomycetes	Hypocreales	Nectriaceae	Fusarium	2	Plant pathogen	0.57a	0.78a	0.22b	0.67a
fungi_ASV53	Sordariomycetes	Sordariales	Unidentified	Unidentified	3	Saprotroph	1.06a	0.01b	0.01b	0.01b
fungi_ASV59	Sordariomycetes	Sordariales	Lasiosphaeriaceae	Podospora	4	Saprotroph	0.82a	0.31a	0.01b	0.01b
fungi_ASV34	Sordariomycetes	Glomerellales	Plectosphaerellaceae	Gibellulopsis	4	Plant pathogen	0.10b	0.14b	1.34 a	0.32b
fungi_ASV52	Dothideomycetes	Pleosporales	Pleosporaceae	Alternaria	5	Plant pathogen	0.98a	0.05b	0.08b	0.05b
fungi_ASV46	Sordariomycetes	Xylariales	Microdochiaceae	Microdochium	5	Saprotroph	0.23b	0.07c	0.95a	0.19b
fungi_ASV19	Sordariomycetes	Microascales	Microasaceae	unclassified_ Microasaceae	5	Saprotroph	0.01c	3.52a	0.02c	0.43b
fungi_ASV18	Sordariomycetes	Sordariales	Chaetomiaceae	Botryotrichum	5	Saprotroph	0.44b	1.46a	0.49b	1.55a
fungi_ASV1	Sordariomycetes	Sordariales	Chaetomiaceae	Botryotrichum	5	Saprotroph	3.81d	14.05b	9.6c	18.62a

Lowercase letters indicate significant differences among rotation systems at $P < 0.05$

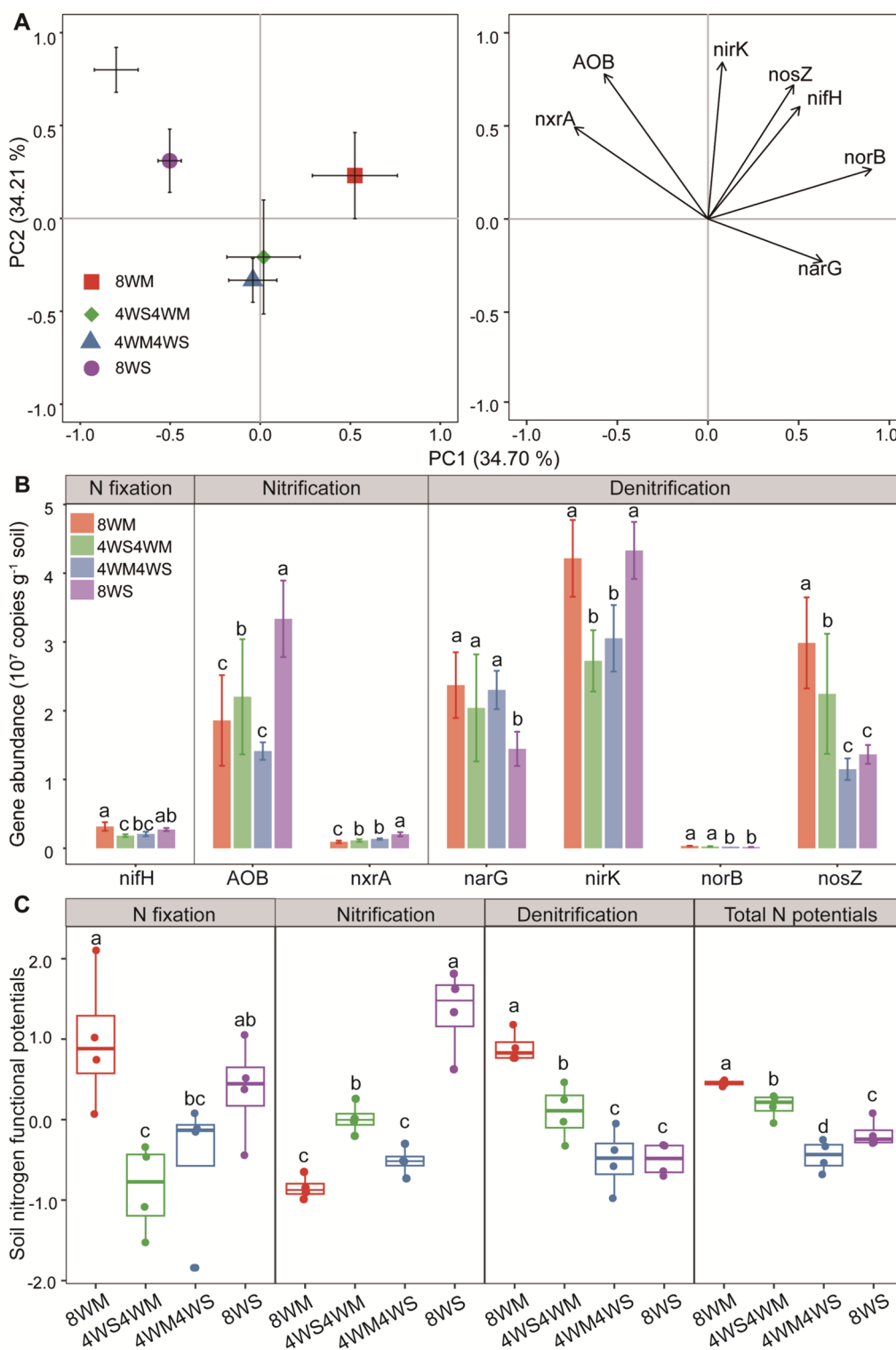


Fig. 4 Soil nitrogen-cycling microbial communities under different cropping systems. **A** First two principal components (PC1 and PC2) of principal component analysis (PCA) using the abundances of seven nitrogen functional genes among the different cropping systems. **B** Quantitative changes of nitrogen functional gene abundances (10^6 copies g^{-1} dry soil) across different cropping systems. **C** Soil nitrogen functional potentials of nitrogen fixation, nitrification, denitrification, and total nitrogen function. Different lowercase letters above the bars indicate significant differences ($P < 0.05$), based on Tukey's HSD test. The average of cropping systems in A is presented as square markers \pm standard error ($n=4$)

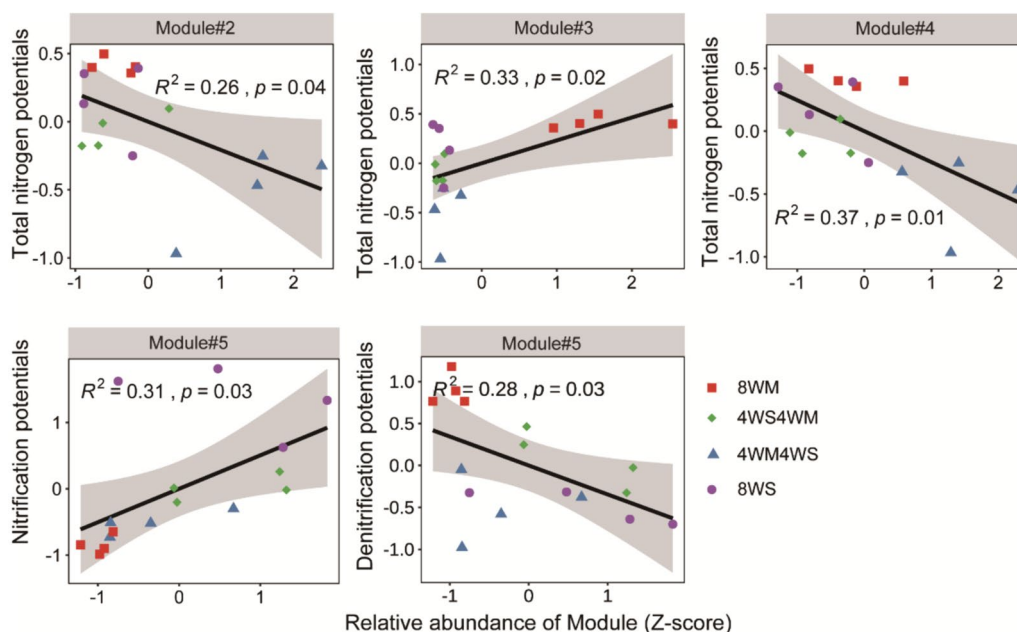


Fig. 5 Regression relationships between the relative abundance of the main modules and soil nitrification, denitrification and total nitrogen potentials

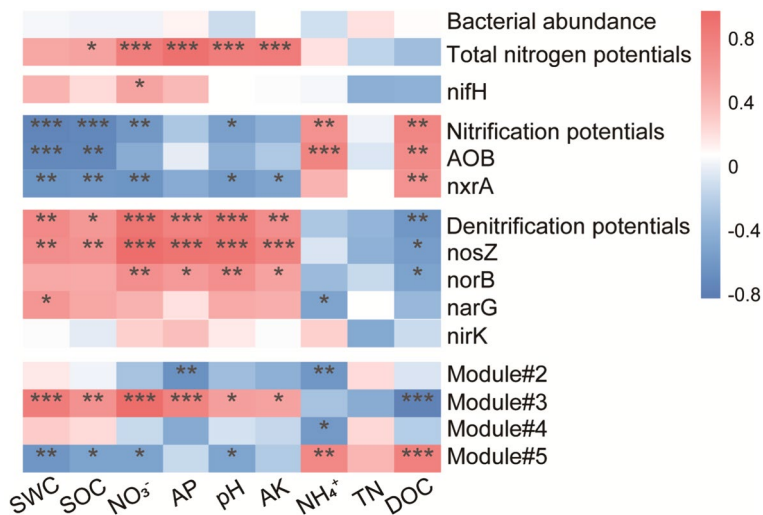


Fig. 6 Heatmaps for Pearson correlation analysis of soil nitrogen function potentials, abundances of nitrogen function genes and network module and soil physicochemical properties. Asterisks indicate significant differences at $P < 0.05$ (*), $P < 0.01$ (**) or $P < 0.001$ (***). Red and green colours represent positive and negative correlations, respectively

analysis (Fig. 6). Relative abundances of Module#3 and Module#5 significantly correlated with more soil physicochemical properties, than those of Module#2 and Module#4. For example, relative abundances of Module#3 positively correlated with SWC, SOC, NO₃⁻, AP, pH and AK, and negatively correlated with DOC. Relative abundances of Module#2 negatively correlated with AP and NH₄⁺, and those of Module#4 only correlated with NH₄⁺.

Soil total nitrogen functional potentials, denitrification potentials, fixed nitrogen and denitrification genes significantly positively correlated with some soil physicochemical properties, whereas nitrification potentials and genes showed the opposite trend. Specifically, soil total nitrogen functional potentials and denitrification potential all positively correlated with SOC, NO₃⁻, AP, pH and AK. The *nifH* positively correlated with NO₃⁻. The *nosZ* and

norB positively correlated with NO_3^- , AP, pH and AK, and negatively correlated with DOC. By contrast, AOB and *nrrA* negatively correlated with SWC, and SOC, and positively correlated with NH_4^+ and DOC.

Linking crop yield to bacterial–fungal network modules and nitrogen function

Under succeeding wheat–maize rotation, maize yield was strongly affected by Module#3 ($P < 0.01$) and Module#5 ($P < 0.05$) based on Mantel test, and was negatively correlated with soil nitrogen fixation potentials ($P < 0.05$) and denitrification potentials ($P < 0.05$), and positively with soil nitrification potentials ($P < 0.05$) based on Pearson correlation analysis (Fig. 7A). Wheat yield was strongly affected by Module#3 ($P < 0.05$), and negatively correlated with soil total nitrogen potentials ($P < 0.05$). Under succeeding wheat–soybean rotation, wheat and soybean yield all showed a significant correlation with Module#2 and Module#4, and a negative and significant correlation with soil nitrification potentials ($P < 0.05$) (Fig. 7B).

Discussion

This study characterized the influence of preceding rotation systems on the bacteria–fungal interactions and nitrogen functional potentials in the wheat–maize and wheat–soybean double cropping system of the North China Plain, and their direct and indirect effects on crop yield. We found the effects of preceding crop rotation on complexity and key modules of bacterial–fungal networks, nitrogen functional genes and potentials were

different in succeeding wheat–maize and wheat–soybean rotation. These changes may be caused by the root exudates or signaling molecules of different crop rotational diversity and previous crop types [24, 25, 52], in turn affects crop productivity of succeeding wheat–maize rotation and wheat–soybean rotation. These findings improve our understanding of how diverse rotation alters the relationships between soil microbial communities and nitrogen cycling functions.

Preceding wheat–soybean effects on soil bacterial–fungal network and nitrogen functional potentials under subsequent wheat–maize rotation

Preceding wheat–soybean rotation (4WS4WM) decreased the soil bacterial and fungal ASV numbers, as well as their interaction network complexity under subsequent wheat–maize rotation, when compared to simple wheat–maize rotation (8WM) (Table 1). This is consistent with previous studies that soybean straw addition into sugarcane/soybean intercropping exhibited lower bacterial and fungal network complexity than no straw [53]. This may be attributed to the inclusion of soybean in the wheat–maize rotation systems increasing generalist microbes through changes to soil properties, carbon inputs and habitat disruptions, which might out-compete specialists and reduce the overall microbial diversity and complexity [53, 54]. Although the complexity of the bacterial–fungal network was reduced in 4WS4WM, it did not affect the role of soil microorganisms in plant

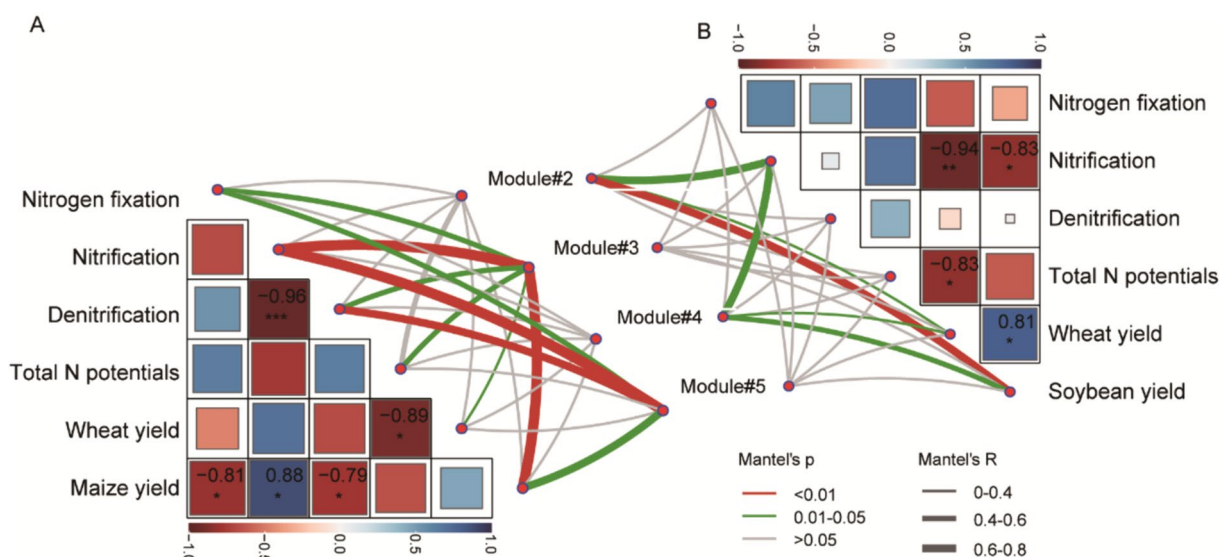


Fig. 7 Relationship between bacterial–fungal network modules, nitrogen functional potentials and crop yield under succeeding 4-year wheat–maize (A) and wheat–soybean rotation (B) according to the Mantel test and Pearson correlation analysis. Nitrogen fixation potentials; Nitrification, nitrification potentials; Denitrification, denitrification potentials; Total N potentials, Total nitrogen potentials

nutrient acquisition and soil fertility because the microbial community was functionally redundant [55].

4WS4WM decreased the relative abundance of Module#3, and increased those of Module#5 compared with 8WM (Fig. 1D). The reduced abundances of Module#3 in 4WS4WM were mainly due to the extinction of many bacterial ASVs in each phylum (Fig. 2), suggesting the decreased diversity of Module#3 in 4WS4WM. This may be closely associated with the soil nutrient status. Relative abundance of Module#3 decreased with decreasing SWC, SOC, NO_3^- , AP, AK and pH, and increasing DOC (Fig. 6). First, the soybean incorporated into the wheat–maize rotation system not only reduce the need for mineral nitrogen fertilizers, but also promote the absorption of soil nitrate, AP and AK for crop growth and accelerated crop residue decomposition [56, 57], which released more soil DOC to soil [58]. Second, the reduced soil available nutrient in 4WS4WM would inhibit the growth of some taxa [59]. The higher Module#5 abundance in 4WS4WM was mainly attributed to the increase in saprotrophic *Botryotrichum* (fungi_ASV1, fungi_ASV18) and *Microasceae* (fungi_ASV19) (Table 2), aligning with findings from legume rotation studies that have reported an enrichment of saprotrophic fungi [60, 61]. In this study, preceding wheat–soybean rotation significantly increased the 4-year maize yield of wheat–maize (Fig. 2S), which meant that more straw returns provided more substrate for saprophytic fungi. The changes in soil properties induced by preceding wheat–soybean rotation directly affect the abundances of Module#3 and Module#5, which ultimately affect the succeeding wheat and maize yield (Figs. 6, 7A). These results suggested previous rotation of wheat and soybean increased crop productivity of the wheat–maize system by increasing the utilization of soil nutrients, decreasing the diversity of Module#3 and optimizing the growth of saprophytic fungi in Module#5 [11, 31].

4WS4WM also decreased the absolute abundances of denitrifying bacteria such as *Rubrobacter* and *Bacillus* in Module#5 compared to 8WM (Fig. 3), which was associated with the decreased soil NO_3^- . The reduced levels of nitrate, which are used as terminal electron acceptors in denitrification, could partly account for the lower abundances of denitrifying *Rubrobacter* and *Bacillus* in the 4WS4WM fields. This was partly supported by the results from the reduced soil denitrification potentials (especially *nirK* and *nosZ* genes) in 4WS4WM (Fig. 4). *Rubrobacter* is known for its ability to grow under extreme conditions, such as high halotolerance, and they carry *nirB*, *norB*, *narG*, and *narH* genes [62, 63]. Some *Bacillus* species play important roles in nitrogen cycling processes like dissimilatory nitrate/nitrite reduction and N_2O emission/reduction through encoding of genes like *nirK* and

nosZ [64, 65]. The *nirK* gene encodes nitrite reductase protein that transforms nitrite into gaseous nitrogen oxides [66], and *nosZ* gene encodes nitrous oxide reductase to the reduction of nitrous oxide [67]. The decrease in abundance of the *nirK* and *nosZ* genes could potentially indicate lower greenhouse gas production and lower conversion of N_2O to N_2 . These findings suggested incorporating soybean into wheat–maize rotations can mitigate soil denitrification potentials and N_2O emissions by regulating key soil microbial modules.

Preceding wheat–maize effect on soil bacterial–fungal network and nitrogen functional potentials under subsequent wheat–soybean rotation

Preceding wheat–maize (4WM4WS) significantly altered microbial ASVs and co-occurrence network under subsequent wheat–soybean rotation, compared with simple wheat–soybean rotation (8WS) (Table 1 and Fig. 1A). Specifically, bacterial ASVs and bacterial–fungal network nodes decreased under 4WM4WS. This may be because the addition of maize in wheat–soybean rotation increases the variety and frequency of crop rotation and alters soil nutrient status, resulting in a decline in the living conditions of some bacterial species [14]. This study also showed that 4WM4WS increased the positive interaction between bacteria and the overall bacterial–fungal network complexity. This may mean that under the influence of maize as an intermediate crop, closer cooperative relationships are formed within the soil bacterial community. Some bacteria may be rewarded by secreting substances that favors the growth of others, forming a more stable mutualistic network [68]. On the whole, although the species of soil bacteria decreased after maize conversion, the enhancement of bacterial cooperation network may be conducive to the stability of soil microecosystem.

Compared to 8WS, 4WM4WS mainly increased the Module#2 relative abundance by increasing the bacterial species belonging to Actinobacteria, Proteobacteria, Acidobacteria, Chloroflexi, and Gemmatimonas (Figs. 1, 2), which was in line with Module#3 under 4WS4WM. Interestingly, Module#2 also had the highest number of nodes among the network modules (Fig. 2), suggesting an increase in the diversity of key modules. These findings were consistent with the results of Fan et al. [10], who demonstrated that the biodiversity of key modules was positively associated with wheat production in a 35-year field fertilization experiment. In addition, 4WM4WS increased the relative abundances of Module#4 due to more nitrifying *Nitrosomonadaceae* (*MNDI* and *Ellin6607*) and pathogenic fungi_ASV34 (genus *Gibellulopsis*, 1.34%) compared to 8WS (Fig. 3 and Table 2). *Nitrosomonadaceae* are ammonia-oxidizing bacteria that play an important

role in nitrogen cycling by converting ammonia to nitrite during the first step of nitrification [69]. Their increased abundance under 4WM4WS suggests more rapid nitrification was occurring. This is likely because the 4WM4WS treatment can improve the efficiency of nitrogen fixation in soybean and have higher nitrogen inputs [70], providing more substrate for nitrifiers to oxidize. The increased fungal pathogen *Gibellulopsis* under 4WM4WS can be explained by the biomass of wheat residues and soybean root exudates under the wheat–soybean rotation system. Soybean root exudates, such as phenolic acids, sugars, amino acids, and organic acids, can promote the growth of pathogens in the rhizosphere [71]. 4WM4WS treatment increases crop diversity and residue biomass, and provides rich substrates for the colonization and growth of pathogenic fungi. Bainard et al. [72] also got similar results under rotation with a legume pulse. Main network module of bacteria–fungi directly contributed to the wheat yield by negatively regulating soil physicochemical properties under succeeding wheat–soybean rotation (Fig. 7B). These results indicated the 4WM4WS stimulate more nitrifying *Nitrosomonadaceae* to proliferate, which could contribute to nutrient availability and further increase crop production [73, 74]. In addition, the long-term effects of 4WM4WS on the accumulation of pathogens are needed to further examine sustainable agriculture.

Although increasing nitrifying *Nitrosomonadaceae* abundance in the key network module, 4WM4WS decreased soil nitrification potentials under the subsequent wheat–soybean system (Fig. 4). These results suggested changes in nitrogen functional profiles within individual modules of the microbial network analysis do not necessarily determine the overall soil nitrogen functional potentials. Specifically, the abundances of nitrifier (AOB and *nxrA*) and denitrifiers (*nirK*) were lower, while denitrifying *narG* gene abundance was higher compared to the simple wheat–soybean rotation. This decrease in nitrogen-fixing and transforming microbes could be attributed to the strong nitrogen demand of maize during its growth period, which depleted the available nitrogen sources in soil [75]. At the same time, the relative increase in *narG*, which is involved in nitrite reduction, suggests the soil microbial community may have optimized their nitrogen conversion pathways in response to lower nitrogen availability. We also confirmed the negative correlation between soil nitrogen functional genes, especially *narG*, and soybean yield under succeeding wheat–soybean rotation (Fig. 7B). These findings suggested increasing crop diversity in soybean rotation can not only reduce nitrate accumulation through increased *narG* and decreased

AOB and *nxrA*, but also control the greenhouse gas (e.g. NO and N₂O) emissions through decreased *nirK* gene [76], which improved crop yield ultimately.

Conclusions

In this study, the effects of preceding rotation systems on the bacteria–fungal co-occurrence network complexity and modularity, and nitrogen functional potentials in wheat–maize and wheat–soybean soil were investigated. Our results demonstrated that the crop yield and nitrogen-cycle process were regulated by different ecological clusters in succeeding wheat–maize and wheat–soybean soil. Module#3 with the least species and Module#5 with the most nitrifying and denitrifying bacterial species were more sensitive in the succeeding wheat–maize soil, whereas Module#2 with the most species and Module#4 with the highest abundances of nitrifying bacteria (*Nitrosomonadaceae*) were active in succeeding wheat–soybean soil. The wheat–soybean followed by wheat–maize system increased the nitrification potentials, and decreased the nitrogen fixation and denitrification potentials, which were directly and strongly correlated with the abundances of Module#3 and Module#5, thus improving the utilization of soil nutrients and succeeding maize yield. In contrast, the wheat–maize followed by wheat–soybean system decreased the nitrification potentials through the changes of Module#2 and Module#4, which can reduce soil nitrate accumulation and promote succeeding wheat and soybean yield. These findings significantly facilitate our understanding of microbial nitrogen cycling in diverse agricultural soils and lay a foundation for manipulating specific microorganisms to regulate nitrogen cycling and promote agroecosystem sustainability.

Supplementary Information

The online version contains supplementary material available at <https://doi.org/10.1186/s40538-024-00617-6>.

Supplementary Material 1.

Acknowledgements

Not applicable.

Author contributions

STY contributed to the design of experiments, the acquisition, analysis, or interpretation of data and manuscript writing. TSW and SHY reviewed data curation, investigation and writing. XGC, TSW, SHY and XHP were involved in revising the manuscript. TSW and SHY provided fund acquisition. All authors read and approved the final manuscript.

Funding

This study was financially supported by the National Natural Science Foundation of China (No. 42077099, No. 42107339), and Agriculture Research System of China (No. CARS-04).

Availability of data and materials

The data sets used or analyzed during the current study are available from the corresponding author on reasonable request.

Declarations**Ethics approval and consent to participate**

Not applicable.

Consent for publication

All authors listed have read the complete manuscript and have approved submission of the paper.

Competing interests

The authors declare no competing interests.

Author details

¹National Engineering Research Center of Arable Land Protection, Institute of Agricultural Resources and Regional Planning, Chinese Academy of Agricultural Sciences, Beijing 100081, People's Republic of China. ²College of Water Resources and Civil Engineering, China Agricultural University, Beijing 100083, People's Republic of China.

Received: 18 April 2024 Accepted: 18 July 2024

Published online: 30 July 2024

References

- Tilman D, Balzer C, Hill J, Befort BL. Global food demand and the sustainable intensification of agriculture. *Proc Natl Acad Sci.* 2011;108(50):20260–4. <https://doi.org/10.1073/pnas.1116437108>.
- Feeding the future global population. *Nat Commun.* 2024;15(1): 222. <https://doi.org/10.1038/s41467-023-44588-y>.
- Gan Y, Hamel C, O'Donovan JT, Cutforth H, Zentner RP, Campbell CA, Niu Y, Poppy L. Diversifying crop rotations with pulses enhances system productivity. *Sci Rep.* 2015;5:14625. <https://doi.org/10.1038/srep14625>.
- Tiemann LK, Grandy AS, Atkinson EE, Marin-Spiotta E, McDaniel MD. Crop rotational diversity enhances belowground communities and functions in an agroecosystem. *Ecol Lett.* 2015;18(8):761–71. <https://doi.org/10.1111/ele.12453>.
- Yates F. The analysis of experiments containing different crop rotations. *Biometrics.* 1954;10(3):324–46. <https://doi.org/10.2307/3001589>.
- Zhao J, Yang Y, Zhang K, Jeong J, Zeng Z, Zang H. Does crop rotation yield more in China? A meta-analysis. *Field Crops Res.* 2020. <https://doi.org/10.1016/j.fcr.2019.107659>.
- Zhang K, Maltais-Landry G, Liao HL. How soil biota regulate c cycling and soil c pools in diversified crop rotations. *Soil Biol Biochem.* 2021;156: 108219. <https://doi.org/10.1016/j.soilbio.2021.108219>.
- Fierer N. Embracing the unknown: disentangling the complexities of the soil microbiome. *Nat Rev Microbiol.* 2017;15(10):579–90. <https://doi.org/10.1038/nrmicro.2017.87>.
- Wang G, Li X, Xi X, Cong W-F. Crop diversification reinforces soil microbiome functions and soil health. *Plant Soil.* 2022;476:375–83. <https://doi.org/10.1007/s11104-022-05436-y>.
- Fan K, Delgado-Baquerizo M, Guo X, Wang D, Zhu YG, Chu H. Biodiversity of key-stone phylotypes determines crop production in a 4-decade fertilization experiment. *ISME J.* 2021;15:550–61. <https://doi.org/10.1038/s41396-020-00796-8>.
- Fan K, Delgado-Baquerizo M, Guo X, Wang D, Zhu Y-G, Chu H. Microbial resistance promotes plant production in a four-decade nutrient fertilization experiment. *Soil Biol Biochem.* 2020. <https://doi.org/10.1016/j.soilbio.2019.107679>.
- NBSC, 2023. National Bureau of Statistics-China.
- Wang Y, Ling X, Ma C, Liu C, Zhang W, Huang J, Peng S, Deng N. Can china get out of soy dilemma? A yield gap analysis of soybean in china. *Agron Sustain Dev.* 2023;43(4):47. <https://doi.org/10.1007/s13593-023-00897-6>.
- Bei S, Zhang Y, Li T, Christie P, Li X, Zhang J. Response of the soil microbial community to different fertilizer inputs in a wheat-maize rotation on a calcareous soil. *Agric Ecosyst Environ.* 2018;260:58–69. <https://doi.org/10.1016/j.agee.2018.03.014>.
- Xiao G, Zhao Z, Liang L, Meng F, Wu W, Guo Y. Improving nitrogen and water use efficiency in a wheat-maize rotation system in the north china plain using optimized farming practices. *Agric Water Manag.* 2019;212:172–80. <https://doi.org/10.1016/j.agwat.2018.09.011>.
- Guo JH, Liu XJ, Zhang Y, Shen JL, Han WX, Zhang WF, Christie P, Goulding KW, Vitousek PM, Zhang FS. Significant acidification in major Chinese croplands. *Science.* 2010;327(5968):1008–10. <https://doi.org/10.1126/science.1182570>.
- Kirkegaard JA, Ryan MH. Magnitude and mechanisms of persistent crop sequence effects on wheat. *Field Crop Res.* 2014;164:154–65. <https://doi.org/10.1016/j.fcr.2014.05.005>.
- Ai C, Zhang S, Zhang X, Guo D, Zhou W, Huang S. Distinct responses of soil bacterial and fungal communities to changes in fertilization regime and crop rotation. *Geoderma.* 2018;319:156–66. <https://doi.org/10.1016/j.geoderma.2018.01.010>.
- Song D, Dai X, Guo T, Cui J, Zhou W, Huang S, Shen J, Liang G, He P, Wang X, Zhang S. Organic amendment regulates soil microbial biomass and activity in wheat-maize and wheat-soybean rotation systems. *Agric Ecosyst Environ.* 2022. <https://doi.org/10.1016/j.agee.2022.107974>.
- Agomoh IV, Drury CF, Yang X, Phillips LA, Reynolds WD. Crop rotation enhances soybean yields and soil health indicators. *Soil Sci Soc Am J.* 2021;85(4):1185–95. <https://doi.org/10.1002/saj2.20241>.
- Schmidt JE, Kent AD, Brisson VL, Gaudin ACM. Agricultural management and plant selection interactively affect rhizosphere microbial community structure and nitrogen cycling. *Microbiome.* 2019. <https://doi.org/10.1186/s40168-019-0756-9>.
- Hu X, Liu J, Liang A, Li L, Yao Q, Yu Z, Li Y, Jin J, Liu X, Wang G. Conventional and conservation tillage practices affect soil microbial co-occurrence patterns and are associated with crop yields. *Agric Ecosyst Environ.* 2021. <https://doi.org/10.1016/j.agee.2021.107534>.
- Crotty FV, Fychan R, Sanderson R, Rhymes JR, Bourdin F, Scullion J, Marley CL. Understanding the legacy effect of previous forage crop and tillage management on soil biology, after conversion to an arable crop rotation. *Soil Biol Biochem.* 2016;103:241–52. <https://doi.org/10.1016/j.soilbio.2016.08.018>.
- Azeem M, Sun D, Crowley D, Hayat R, Hussain Q, Ali A, Tahir MI, Jayasundar P, Rinklebe J, Zhang Z. Crop types have stronger effects on soil microbial communities and functionalities than biochar or fertilizer during two cycles of legume-cereal rotations of dry land. *Sci Total Environ.* 2020;715: 136958. <https://doi.org/10.1016/j.scitotenv.2020.136958>.
- Li T, Xie H, Ren Z, Hou Y, Zhao D, Wang W, Wang Z, Liu Y, Wen X, Han J, Mo F, Liao Y. Soil tillage rather than crop rotation determines assembly of the wheat rhizobacterial communities. *Soil Tillage Res.* 2023;226: 105588. <https://doi.org/10.1016/j.still.2022.105588>.
- Venter ZS, Jacobs K, Hawkins H-J. The impact of crop rotation on soil microbial diversity: a meta-analysis. *Pedobiologia.* 2016;59(4):215–23. <https://doi.org/10.1016/j.pedobi.2016.04.001>.
- Jing J, Cong WF, Bezemer TM. Legacies at work: plant-soil-microbiome interactions underpinning agricultural sustainability. *Trends Plant Sci.* 2022. <https://doi.org/10.1016/j.tplants.2022.05.007>.
- Benitez M-S, Ewing PM, Osborne SL, Lehman RM. Rhizosphere microbial communities explain positive effects of diverse crop rotations on maize and soybean performance. *Soil Biol Biochem.* 2021;159: 108309. <https://doi.org/10.1016/j.soilbio.2021.108309>.
- Grayston SJ, Wang S, Campbell CD, Edwards AC. Selective influence of plant species on microbial diversity in the rhizosphere. *Soil Biol Biochem.* 1998;30(3):369–78. [https://doi.org/10.1016/S0038-0717\(97\)00124-7](https://doi.org/10.1016/S0038-0717(97)00124-7).
- Xie Y, Dong C, Chen Z, Liu Y, Zhang Y, Gou P, Zhao X, Ma D, Kang G, Wang C, Zhu Y, Guo T. Successive biochar amendment affected crop yield by regulating soil nitrogen functional microbes in wheat-maize rotation farmland. *Environ Res.* 2021;194: 110671. <https://doi.org/10.1016/j.envres.2020.110671>.
- Yu S, Wang T, Meng Y, Yao S, Wang L, Zheng H, Zhou Y, Song Z, Zhang B. Leguminous cover crops and soya increased soil fungal diversity and suppressed pathotrophs caused by continuous cereal cropping. *Front Microbiol.* 2022;13: 993214. <https://doi.org/10.3389/fmicb.2022.993214>.
- Linton NF, Ferrari Machado PV, Deen B, Wagner-Riddle C, Dunfield KE. Long-term diverse rotation alters nitrogen cycling bacterial groups and

- nitrous oxide emissions after nitrogen fertilization. *Soil Biol Biochem.* 2020. <https://doi.org/10.1016/j.soilbio.2020.107917>.
33. Yu T, Nie J, Zang H, Zeng Z, Yang Y. Peanut-based rotation stabilized diazotrophic communities and increased subsequent wheat yield. *Microb Ecol.* 2023;86(4):2447–60. <https://doi.org/10.1007/s00248-023-02254-2>.
 34. Li R, Ren C, Wu L, Zhang X, Mao X, Fan Z, Cui W, Zhang W, Wei G, Shu D. Fertilizing-induced alterations of microbial functional profiles in soil nitrogen cycling closely associate with crop yield. *Environ Res.* 2023. <https://doi.org/10.1016/j.envres.2023.116194>.
 35. Wang G, Liang Y, Zhang Q, Jha SK, Gao Y, Shen X, Sun J, Duan A. Mitigated ch₄ and n₂o emissions and improved irrigation water use efficiency in winter wheat field with surface drip irrigation in the north china plain. *Agric Water Manag.* 2016;163:403–7. <https://doi.org/10.1016/j.agwat.2015.10.012>.
 36. Wang L, Wang T, Yao S, Sun H, Zhang B. Soil compaction development facilitated the decadal improvement of the root system architecture and rhizosphere soil traits of soybean in the north china plain. *Soil Tillage Res.* 2024. <https://doi.org/10.1016/j.still.2023.105983>.
 37. Yan H, Shang A, Peng Y, Yu P, Li C. Covering middle leaves and ears reveals differential regulatory roles of vegetative and reproductive organs in root growth and nitrogen uptake in maize. *Crop Sci.* 2011;51(1):265–72. <https://doi.org/10.2135/cropsci2010.03.0180>.
 38. Wang D, Yi W, Zhou Y, He S, Tang L, Yin X, Zhao P, Long G. Intercropping and n application enhance soil dissolved organic carbon concentration with complicated chemical composition. *Soil Tillage Res.* 2021. <https://doi.org/10.1016/j.still.2021.104979>.
 39. Kalra Y, Crumbaugh J, Maynard D. Nitrate and exchangeable ammonium nitrogen. In: Carter M, Gregorich E, editors. *Soil sampling and methods of analysis*, Second Edition. CRC Press; 2007. <https://doi.org/10.1201/9781420005271.ch6>.
 40. Olsen SR. Estimation of available phosphorus in soils by extraction with sodium bicarbonate. *Misc Paper Inst Agric Res.* 1954;939:1–29.
 41. Holtz JT. *Soil analysis handbook of reference methods*. Boca Raton: Crc Press; 1999.
 42. Callahan BJ, McMurdie PJ, Rosen MJ, Han AW, Johnson AJA, Holmes SP. Dada2: high-resolution sample inference from illumina amplicon data. *Nat Methods.* 2016;13(7):581–3. <https://doi.org/10.1038/nmeth.3869>.
 43. Langfelder P, Horvath S. Wgcna: an r package for weighted correlation network analysis. *BMC Bioinform.* 2008;9(1):559. <https://doi.org/10.1186/1471-2105-9-559>.
 44. Bastian M, Heymann S, Jacomy M. 2009. Gephi: An open source software for exploring and manipulating networks. *Proceedings of the Third International Conference on Weblogs and Social Media, ICWSM 2009, San Jose, California, USA, May 17–20, 2009*.
 45. Delgado-Baquerizo M, Reith F, Dennis PG, Hamonts K, Powell JR, Young A, Singh BK, Bissett A. Ecological drivers of soil microbial diversity and soil biological networks in the southern hemisphere. *Ecology.* 2018;99(3):583–96. <https://doi.org/10.1002/ecy.2137>.
 46. Louca S, Parfrey LW, Doebeli M. Decoupling function and taxonomy in the global ocean microbiome. *Science.* 2016;353(6305):1272. <https://doi.org/10.1126/science.aaf4507>.
 47. Nguyen NH, Song Z, Bates ST, Branco S, Tedersoo L, Menke J, Schilling JS, Kennedy PG. Funguild: an open annotation tool for parsing fungal community datasets by ecological guild. *Fungal Ecol.* 2016;20:241–8. <https://doi.org/10.1016/j.funeco.2015.06.006>.
 48. Yang L, Lou J, Wang H, Wu L, Xu J. Use of an improved high-throughput absolute abundance quantification method to characterize soil bacterial community and dynamics. *Sci Total Environ.* 2018;633:360–71. <https://doi.org/10.1016/j.scitotenv.2018.03.201>.
 49. Gower J. Some distance properties of latent root and vector methods used in multivariate analysis. *Biometrika.* 1966;53(3–4):325–38. <https://doi.org/10.2307/2333639>.
 50. Strom N, Hu W, Haarith D, Chen S, Bushley K. Interactions between soil properties, fungal communities, the soybean cyst nematode, and crop yield under continuous corn and soybean monoculture. *Appl Soil Ecol.* 2020;147: 103388. <https://doi.org/10.1016/j.apsoil.2019.103388>.
 51. Diniz-Filho JA, Soares TN, Lima JS, Dobrovolski R, Landeiro VL, de Campos Telles MP, Rangel TF, Bini LM. Mantel test in population genetics. *Genet Mol Biol.* 2013;36(4):475–85. <https://doi.org/10.1590/s1415-4757201300400002>.
 52. Benitez MS, Osborne SL, Lehman RM. Previous crop and rotation history effects on maize seedling health and associated rhizosphere microbiome. *Sci Rep.* 2017;7(1):15709. <https://doi.org/10.1038/s41598-017-15955-9>.
 53. Zhang T, Liu Y, Ge S, Peng P, Tang H, Wang J. Sugarcane/soybean intercropping with reduced nitrogen addition enhances residue-derived labile soil organic carbon and microbial network complexity in the soil during straw decomposition. *J Integr Agric.* 2024. <https://doi.org/10.1016/j.jia.2024.02.020>.
 54. Yin C, Jones KL, Peterson DE, Garrett KA, Hulbert SH, Paulitz TC. Members of soil bacterial communities sensitive to tillage and crop rotation. *Soil Biol Biochem.* 2010;42(12):2111–8. <https://doi.org/10.1016/j.soilbio.2010.08.006>.
 55. Wagg C, Schlaeppli K, Banerjee S, Kuramae EE, van der Heijden MGA. Fungal-bacterial diversity and microbiome complexity predict ecosystem functioning. *Nat Commun.* 2019;10(1):4841. <https://doi.org/10.1038/s41467-019-12798-y>.
 56. Lee S, Yeo I-Y, Sadeghi AM, McCarty GW, Hively WD, Lang MW. Impacts of watershed characteristics and crop rotations on winter cover crop nitrate-nitrogen uptake capacity within agricultural watersheds in the chesapeake bay region. *PLoS ONE.* 2016;11(6): e0157637. <https://doi.org/10.1371/journal.pone.0157637>.
 57. Kalburtji KL, Mamolos AP. Maize, soybean and sunflower litter dynamics in two physicochemically different soils. *Nutr Cycl Agroecosyst.* 2000;57(3):195–206. <https://doi.org/10.1023/A:1009814218516>.
 58. Hao X, Han X, Wang S, Li L-J. Dynamics and composition of soil organic carbon in response to 15 years of straw return in a mollisol. *Soil Tillage Res.* 2022;215: 105221. <https://doi.org/10.1016/j.still.2021.105221>.
 59. Yang Z, Zhu Q, Zhang Y, Jiang P, Wang Y, Fei J, Rong X, Peng J, Wei X, Luo G. Soil carbon storage and accessibility drive microbial carbon use efficiency by regulating microbial diversity and key taxa in intercropping ecosystems. *Biol Fertil Soils.* 2024;60(3):437–53. <https://doi.org/10.1007/s00374-024-01804-1>.
 60. Schmidt R, Mitchell J, Scow K. Cover cropping and no-till increase diversity and symbiotroph: saprotroph ratios of soil fungal communities. *Soil Biol Biochem.* 2019;129:99–109. <https://doi.org/10.1016/j.soilbio.2018.11.010>.
 61. Borrell AN, Shi Y, Gan Y, Bainard LD, Germida JJ, Hamel C. Fungal diversity associated with pulses and its influence on the subsequent wheat crop in the Canadian prairies. *Plant Soil.* 2016;414(1–2):13–31. <https://doi.org/10.1007/s11104-016-3075-y>.
 62. Ye H, Zhao Y, He S, Wu Z, Yue M, Hong M. Metagenomics reveals the response of desert steppe microbial communities and carbon-nitrogen cycling functional genes to nitrogen deposition. *Front Microbiol.* 2024. <https://doi.org/10.3389/fmicb.2024.1369196>.
 63. Freed S, Ramaley RF, Kyndt JA. Whole-genome sequence of the novel rubrobacter taiwanensis strain yellowstone, isolated from yellowstone national park. *Microbiol Resour Announc.* 2019. <https://doi.org/10.1128/mra.00287-00219>.
 64. Mania D, Heylen K, van Spanning RJ, Frostegård Å. The nitrate-ammonifying and nosz-carrying bacterium *Bacillus acillus vireti* is a potent source and sink for nitric and nitrous oxide under high nitrate conditions. *Environ Microbiol.* 2014;16(10):3196–210. <https://doi.org/10.1111/1462-2920.12478>.
 65. Yoon S, Heo H, Han H, Song D-U, Bakken LR, Frostegård Å, Yoon S. Suggested role of nosz in preventing n₂o inhibition of dissimilatory nitrite reduction to ammonium. *MBio.* 2023;14(5):e01540-e11523. <https://doi.org/10.1128/mbio.01540-23>.
 66. Azziz G, Monza J, Etchebehere C, Irisarri P. Nirs- and nirk-type denitrifier communities are differentially affected by soil type, rice cultivar and water management. *Eur J Soil Biol.* 2017;78:20–8. <https://doi.org/10.1016/j.ejsobi.2016.11.003>.
 67. Orellana LH, Rodriguez-R LM, Higgins S, Chee-Sanford JC, Sanford RA, Ritalahti KM, Löffler FE, Konstantinidis KT. Detecting nitrous oxide reductase (nosz) genes in soil metagenomes: method development and implications for the nitrogen cycle. *MBio.* 2014;5(3): e01193. <https://doi.org/10.1128/mBio.01193-14>.
 68. Wang Y, Zhang H, Zhang Y, Fei J, Xiangmin R, Peng J, Luo G. Crop rotation-driven changes in rhizosphere metabolite profiles regulate soil microbial diversity and functional capacity. *Agric Ecosyst Environ.* 2023. <https://doi.org/10.1016/j.agee.2023.108716>.

69. Prosser J., Head I., Stein L., 2013. The family nitrosomonadaceae. The Prokaryotes: Alphaproteobacteria and Betaproteobacteria, 901–918. https://doi.org/10.1007/978-3-642-30197-1_372.
70. Vanotti MB, Bundy LG. Soybean effects on soil nitrogen availability in crop rotations. *Agron J.* 1995;87(4):676–80.
71. Bai L, Cui J, Jie W, Cai B. Analysis of the community compositions of rhizosphere fungi in soybeans continuous cropping fields. *Microbiol Res.* 2015;180:49–56. <https://doi.org/10.1016/j.micres.2015.07.007>.
72. Bainard LD, Navarro-Borrell A, Hamel C, Braun K, Hanson K, Gan Y. Increasing the frequency of pulses in crop rotations reduces soil fungal diversity and increases the proportion of fungal pathotrophs in a semiarid agroecosystem. *Agric Ecosyst Environ.* 2017;240:206–14. <https://doi.org/10.1016/j.agee.2017.02.020>.
73. Fan S, Zuo J, Dong H. Changes in soil properties and bacterial community composition with biochar amendment after six years. *Agronomy.* 2020;10(5):746. <https://doi.org/10.3390/agronomy10050746>.
74. Zhou G, Fan K, Gao S, Chang D, Li G, Liang T, Liang H, Li S, Zhang J, Che Z, Cao W. Green manuring relocates microbiomes in driving the soil functionality of nitrogen cycling to obtain preferable grain yields in thirty years. *Sci China Life Sci.* 2023;67(3):596–610. <https://doi.org/10.1007/s11427-023-2432-9>.
75. Ordóñez RA, Archontoulis SV, Martínez-Feria R, Hatfield JL, Wright EE, Castellano MJ. Root to shoot and carbon to nitrogen ratios of maize and soybean crops in the us midwest. *Eur J Agron.* 2020;120: 126130. <https://doi.org/10.1016/j.eja.2020.126130>.
76. Hao J, Feng Y, Wang X, Yu Q, Zhang F, Yang G, Ren G, Han X, Wang X, Ren C. Soil microbial nitrogen-cycling gene abundances in response to crop diversification: a meta-analysis. *Sci Total Environ.* 2022;838(4): 156621. <https://doi.org/10.1016/j.scitotenv.2022.156621>.

Publisher's Note

Springer Nature remains neutral with regard to jurisdictional claims in published maps and institutional affiliations.